LOCAL TRANSPORT IN TOKAMAKS WITH OHMIC AND INJECTION HEATING

G. Becker

Max-Planck-Institut für Plasmaphysik
EURATOM Association, D-8046 Garching

Abstract: The anomalous electron heat diffusivity χ_e is investigated by a power scan of the injection heating and by the time evolution of L (low confinement) discharges. It is shown that deviations from the ohmic scaling occur if the non-ohmic electron heating locally exceeds the ohmic power density. The change in scaling is attributed to the injection heating with its different dependence on the plasma parameters rather than to other instabilities or saturation effects. Constraints on χ_e are derived from the electron and ion energy equations and the shape of the measured electron temperature profiles. For small injection power complex χ_e scalings result which cannot be represented by superposing the ohmic and L scalings.

Introduction: As reliable microinstability-based diffusivities are not available at present for tokamaks with ohmic and auxiliary heating, preference is given to empirical scalings determined by means of transport modelling of many series of discharges. The flux-surface-averaged electron heat diffusivity χ_e and the diffusion coefficient D exhibit a scaling in injection-heated plasmas which greatly differs from that with ohmic heating /1-4/. It was demonstrated that the ohmic transport scaling is not a universal plasma quality which is independent of the heating method. One possible explanation for the different scaling is that neutral injection changes the transport mechanism, i.e. the underlying instabilities and/or saturation effects. There might exist a threshold parameter which distinguishes between the confinement regimes. Another possibility is that the transport mechanism itself remains unchanged and the χ_e scaling is modified by the injection heating with its different variation with the plasma parameters. These questions will be pursued by studying the transition between ohmic and L transport and by following the time evolution of L discharges /5/. The paper deals with the anomalous transport in the ohmic, L and intermediate regimes. Results from transport computations (with the BALDUR code /6,7/) are used.

Constraints on χ_e with ohmic and injection heating: The steady-state electron and ion energy equations and measured T_e profile shapes are used to derive constraints for the electron heat diffusivity. In the stationary ohmic and neutral-beam-heated phases of ASDEX characteristic shapes of $T_e(r)$ are observed. This is illustrated by Fig. 1, which shows an example of the time evolution of the electron temperature profile in an L discharge with an injection period of 4C0 ms and an absorbed beam power P_{abs} = 2.0 MW. As can be seen, a Gaussian shape is found during the stationary ohmic phase. After the beginning of neutral injection (t_{on} = 1.12 s), the T_e profile changes to an approximately triangular shape which is then maintained during the whole injection period. The 'confinement zone' (hatched in Fig.1) is defined by $r_{q=1} < r < 0.9a$, where the plasma radius a is equal to the separatrix radius of 40cm.

Neglecting the ion heat conduction, the steady-state electron and ion energy equations yield

$$\frac{1}{r}\frac{d}{dr}\left(rn\,\chi_e\,\frac{dT_e}{dr}\right) + \eta j_t^2 + P_b \approx 0 \qquad (1)$$

with $\eta j_t^2 = E_t j_t$. The power density of the ASDEX neutral injection system can be approximated by $P_b(r) = \alpha_b/r$ with $\alpha_b = P_{abs}/(4\pi^2 R_o a)$ and major radius R_o. After integration it follows that

$$\chi_e(r) = \left[\frac{c}{4\pi} E_t B_p(r) + \alpha_b\right] n(r)^{-1} \left|\frac{dT_e}{dr}\right|^{-1} . \qquad (2)$$

With $P_b = 0$ and $T_e(r) = T_e(0)\exp(-\alpha r^2/a^2)$ one obtains the constraint

$$\chi_e^{OH}(r) = \frac{c}{8\pi}\,\frac{a^2}{\alpha}\,E_t\,\frac{B_p(r)}{rn(r)T_e(r)} . \qquad (3)$$

Large injection power and $T_e(r) \simeq T_e(0)(1-r/a)$ yield the constraint

$$\chi_e^{L}(r) \simeq a\,\alpha_b\,T_e(0)^{-1}\,n(r)^{-1} . \qquad (4)$$

Comparing the constraints shows that the χ_e scalings depend on the heating method and its variation with the plasma parameters. Neutral injection does not introduce a $B_p(r)$ dependence in contrast to ηj_t^2. Owing to $j_t(r) \sim T_e(r)^{3/2}$ the ohmic heating and electron temperature profiles are stongly coupled, whereas $P_b(r)$ depends on the target density and injection energy. It is obvious from Eq. (2) that the transport in the intermediate range cannot simply be represented by superposing the ohmic and L scalings, but that rather complex, mixed χ_e scalings occur. The beam heating modifies the ohmic contribution by changing E_t and the T_e profile shape and the ohmic heating modifies the beam contribution.

Transition between ohmic and L transport: The confinement in the intermediate range between OH and L scaling is studied by simulating a series of discharges at $\bar{n} = 2.5 \times 10^{13}$ cm^{-3}, $I_p = 380$ kA, $Z_{eff} = 1.5$ and $P_{OH} = 0.52$ MW with various injection powers. Figure 2 shows the increase of the electron heat diffusivity with rising absorbed beam power. Obviously, at small P_{abs} equal to 0.3 and 0.6 MW the χ_e values clearly exceed the ohmic result (cross) in the middle of the confinement zone at $r = 2a/3$. This explains the observed decrease of the global energy confinement time τ_E /2/. The χ_e profiles with ohmic heating and $P_{abs} = 0.6$ MW are presented in Fig. 3. Special attention is paid to the local ratio of the injection and ohmic heating power densities. Results for various absorbed beam powers are shown in Fig. 4. It is obvious that $P_b/(\eta j_t^2) \simeq 0.3$, where the influence of beam heating should become important, is already exceeded with $P_{abs} = 0.3$ MW. As shown above, the corresponding χ_e and τ_E are indeed found to deviate from the ohmic scaling. With $P_{abs} = 0.6$ and 0.9 MW, neutral injection becomes dominant in the confinement zone. This explains the observed fast transition of τ_E to the L scaling. For $P_{abs} \gtrsim 1.2$ MW the beam power density is large compared with ηj_t^2, which agrees with the essentially pure L confinement found. The power scan shows that the transition to the L regime correlates with the ratio $P_b/(\eta j_t^2)$. Both the deviation from the ohmic scaling and the approach to the L confinement occur at power density ratios which agree with the expected values. According to the electron energy equation, injection powers of this level perturb the ohmic state. The associated change in

confinement suggests that the χ_e scaling responds to the auxiliary heating. The fact that the coupling between the ohmic heating profile and $T_e(r)$ is broken up with neutral injection should play an important role. As the smallest injection power scarcely modifies the plasma parameters, such as density and temperature gradients and poloidal beta, a transition to other instabilities and/or saturation effects, i.e. to a different transport mechanism, is very unlikely.

Transport behaviour after neutral injection: A characteristic time development of the diffusivities χ_e and D in L discharges was found by means of transport simulations /1,2/. It was shown that the L phase persists for about 100 ms after the end of injection. As the slowing-down time of the fast beam ions is only about 10 ms, the injection power rapidly decays. It is thus concluded that the L transport does not require the presence of injection heating, beam fuelling and direct ion heating. Simulations of many L discharges revealed that the phase with the ion-electron energy transfer rate $P_{ie} > 0$ also lasts for a time span of about 100 ms, which suggests that the L phase is maintained by non-ohmic electron heating.

The time development of the electron temperature profiles measured after injection is shown in Fig. 5. Although the beam power is negligibly small, the Gaussian-shaped T_e profiles typical of the ohmic phase are only reached after about 80 ms. The central steepening of the profiles results from the electron heating due to P_{ie}, which is largest in the plasma centre. Profiles of $P_{ie}/(nj_t^2)$ after neutral injection which were determined by simulating the L discharge with P_{abs} = 2.1 MW in Figs. 2 and 4 are presented in Fig. 6. The absorbed beam power is negligibly small at $t-t_{off}$ = 43 ms, so that the only non-ohmic heating is due to P_{ie}. Owing to P_{ie} a transport scaling different from the ohmic one should thus persist in a considerable fraction of the plasma cross-section. Close to the end of the L phase, however, the ratio of the power densities has become so small that the scaling becomes almost purely ohmic. It is concluded that deviations from the ohmic scaling occur if the non-ohmic electron heating (due to neutral injection or ion-electron energy transfer) locally exceeds the ohmic power density.

References

/1/ Becker, G., ASDEX Team, Neutral Injection Team, Nucl. Fusion 22 (1982) 1589.
/2/ Becker, G., Campbell, D., Eberhagen, A., Gehre, O., Gernhardt, J., et al., Nucl. Fusion 23 (1983) 1293.
/3/ Becker, G., Nucl. Fusion 24 (1984) 1364.
/4/ Kaye, S.M., Goldston, R.J., Bell, M., Bol, K., Bitter, M., et al., Nucl. Fusion 24 (1984) 1303.
/5/ Becker, G., Report IPP III/109 (1986).
/6/ Post, D.E., Singer, C.E., McKenney, A.M., BALDUR: A One-dimensional Plasma Transport Code, PPPL Transport Group, TFTR Physics Group, Report 33 (1981).
/7/ Becker, G., ASDEX Team, Neutral Injection Team, Report IPP III/98 (1984).

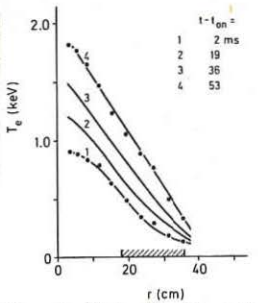

Fig. 1: $T_e(r,t)$ after the beginning of neutral injection (t_{on} = 1.12 s) measured by multi-pulse Thomson scattering in an L discharge with $\bar{n}$ = 2.4 x 10^{13} cm^{-3}, I_p = 280 kA and P_{abs} = 2.0 MW. The hatched area denotes the confinement zone.

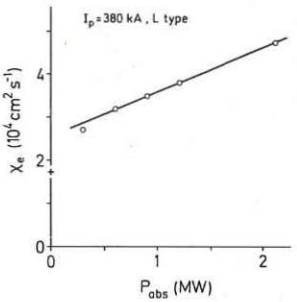

Fig. 2: Approximately homogeneous electron thermal diffusivity from simulations versus absorbed beam power ($\bar{n}$ = 2.5 x 10^{13} cm^{-3}). For comparison, the ohmic χ_e (2a/3) value (cross) is shown.

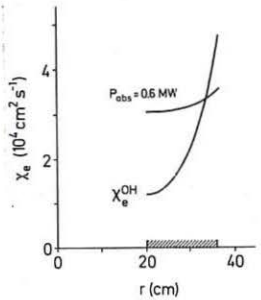

Fig. 3: $\chi_e(r)$ in the confinement zone (hatched) with ohmic heating and neutral-beam heating with two sources.

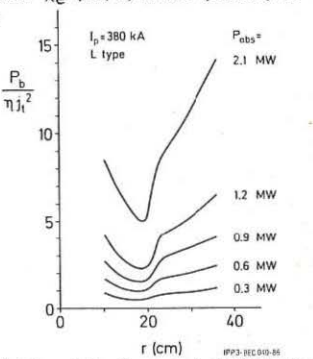

Fig. 4: Ratio of the beam and ohmic power densities versus radius from simulations of the power scan of Fig. 2.

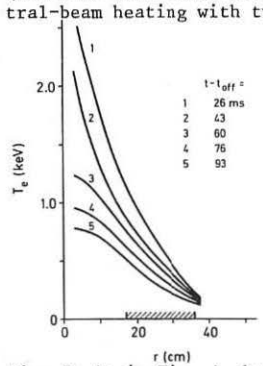

Fig. 5: As in Fig. 1, but after the end of neutral injection (t_{off} = 1.52 s).

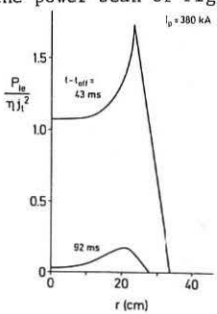

Fig. 6: Ratio of the power densities of ion-electron energy transfer and ohmic heating versus radius after t_{off}.